Responses of Reconstructed Human Epidermis to *Trichophyton rubrum* Infection and Impairment of Infection by the Inhibitor PD169316

Emilie Faway[1], Ludivine Cambier[2], Evelyne De Vuyst[1], Céline Evrard[1], Marc Thiry[3], Catherine Lambert de Rouvroit[1], Bernard Mignon[2] and Yves Poumay[1]

Despite the threatening incidence of dermatophytosis, information is still lacking about the consequences of infection on epidermal barrier functions and about the keratinocyte responses that alert immune components. To identify the mechanisms involved, arthroconidia of the anthropophilic dermatophyte *Trichophyton rubrum* were prepared to infect reconstructed human epidermis (RHE) in vitro. Integrity of the barrier was monitored during infection by measurements of transepithelial electrical resistance and dye-permeation through the RHE. Expression and release of pro-inflammatory cytokines and antimicrobial peptides by keratinocytes inserted into the RHE were assessed, respectively, by quantitative reverse transcriptase–PCR (to analyze mRNA content in tissue extracts) and by ELISA (to detect proteins in culture media). Results reveal that infection by *T. rubrum* is responsible for disruption of the epidermal barrier, including loss of functional tight junctions. It additionally causes simultaneous expression and release of cytokines and antimicrobial peptides by keratinocytes. Potential involvement of the p38 mitogen-activated protein kinase signaling pathway was evaluated during infection by targeted inhibition of its activity. Intriguingly, among several p38 mitogen-activated protein kinase inhibitors, PD169316 alone was able to inhibit growth of *T. rubrum* on Sabouraud agar and to suppress the process of infection on RHE. This suggests that PD169316 acts on a specific target in dermatophytes themselves.

Journal of Investigative Dermatology (2019) ■, ■–■; doi:10.1016/j.jid.2019.03.1147

INTRODUCTION

Dermatophytosis is a superficial mycosis, whose prevalence is estimated between 20 and 25% in the global human population and has increased over the last decade (Havlickova et al., 2008; Hayette and Sacheli, 2015; Seebacher et al., 2008; Zhan and Liu, 2017). The anthropophilic *Trichophyton rubrum* species is the most common dermatophyte responsible for glabrous skin infections (Lee et al., 2015; Tomoyuki et al., 2014), which are generally limited to the stratum corneum (SC) (Weitzman and Summerbell, 1995). The confinement of fungal hyphae and spores in superficial epidermal layers is thought to be associated with both the epidermal barrier itself and the appropriate activation of the immune system (Martinez-Rossi et al., 2017; Mignon et al., 2008; Vermout et al., 2008). The latter is known to induce not only innate immune responses but also an adaptive immune response involving TCR-mediated immunity, which is critical for fungal clearance and clinical recovery (Burstein et al., 2018; Calderon and Hay, 1984; Heinen et al., 2018). However, the consequences of dermatophytic infection on the epidermal barrier and on the keratinocyte responses that alert innate immune components remain poorly understood.

The epidermal barrier protects the organism against external aggressions and water loss (Bäsler et al., 2016). Its efficiency is possible because of the collaboration between its physical components, that is, the SC and tight junctions (TJs), antimicrobial peptides (AMPs), cells of the immune system, and the skin microbiome (Brandner, 2016; Proksch et al., 2008). The SC is composed of corneocytes held together by corneodesmosomes across the intercellular lipid matrix and is extremely resistant to physical stress, as well as relatively impermeable to water and many chemicals (Haftek, 2015; van Smeden and Bouwstra, 2016). TJs are intercellular junctions established between granular keratinocytes and are responsible for the paracellular impermeability in the epidermis (Kirschner et al., 2013).

In case of infection, keratinocytes are the cells initially encountered by dermatophytes. They can detect pathogens via pathogen-associated molecular pattern recognition, by using pattern recognition receptors: toll-like receptors (TLRs) 2, 4, and 6, notably (Brasch et al., 2014; Cambier et al., 2016; García-Madrid et al., 2011). Activation of pattern recognition receptors on keratinocytes induces signaling pathways, leading to expression and release of pro-

[1]URPHYM-NARILIS, University of Namur, Namur, Belgium; [2]FARAH, Faculty of Veterinary Medicine, University of Liège, Liège, Belgium; and [3]Cell and Tissue Biology Unit, GIGA–Neurosciences, University of Liège, Liège, Belgium

Correspondence: Yves Poumay, URPHYM-NARILIS, University of Namur, 61 rue de Bruxelles, B-5000 Namur, Belgium. E-mail: yves.poumay@unamur.be

Abbreviations: AMP, antimicrobial peptide; CN, copy number; hBD, human β-defensin; MAPK, mitogen-activated protein kinase; PBS, phosphate buffered saline; RHE, reconstructed human epidermis; SC, stratum corneum; TJ, tight junction; TLR, toll-like receptor; TNF, tumor necrosis factor

Received 21 December 2018; revised 22 March 2019; accepted 25 March 2019; accepted manuscript published online 12 April 2019; corrected proof published online XXX

inflammatory cytokines and AMP. Particularly, the p38 mitogen-activated protein kinase (MAPK) signaling pathway can be activated in response to environmental stresses and its involvement is implied in a variety of cellular processes, including inflammation (Kyriakis and Avruch, 2012; Zarubin and Han, 2005). Interestingly, the p38 MAPK signaling pathways were involved in AMP expression by keratinocytes exposed to a cell wall component of *Candida albicans* (Li et al., 2011) and were found to be activated in keratinocytes exposed to *Trichophyton equinum* dermatophytes (Achterman et al., 2015). Moreover, several studies performed in vitro on keratinocyte monolayers have shown increased expression and release of cytokines, such as tumor necrosis factor(TNF)-α, IL-1α, IL-1β, IL-6, and IL-8, in response to stimulation by dermatophytes (Nakamura et al., 2002; Shiraki et al., 2006; Tani et al., 2007).

In addition, the exposure of keratinocytes cultured as monolayers to fungal cells is poorly representative of in vivo infection. In vivo models of dermatophytosis using guinea pigs (Baldo et al., 2010) or mice (Cambier et al., 2014; Heinen et al., 2018) are useful to study the immune responses against dermatophytosis, but differences could exist with human infection. Therefore, cultures of human skin equivalents appear to be quite relevant models to study human dermatophytosis.

Such a model of dermatophytosis was setup through infection of reconstructed human epidermis (RHE) by arthroconidia of the anthropophilic species *T. rubrum* (Faway et al., 2017). This model appears rather representative of human dermatophytosis, with fungal components proliferating over time and invading the SC. Herein, this model has been used in order to assess damage to the epidermal barrier, as well as to detect specific activation of keratinocyte responses during infection. While investigating the potential involvement of the p38 MAPK signaling pathway in the reported keratinocyte responses to infection, the unique effects of PD169316 compound were highlighted on growth and infection properties of dermatophytes—PD169316 compound being a well-known inhibitor of p38 MAPK.

RESULTS

Fungal hyphae invaded the SC by progressing between corneocytes

Progression of fungal elements through RHE infected by *T. rubrum* arthroconidia was monitored over time by morphological analysis (Figure 1a). A progressive invasion into SC was observed: on the first day, hyphae emerging from arthroconidia spread over the SC surface and penetrated SC by sneaking between corneocytes (Figure 1b); on the fourth day, hyphae were found in the intercellular space through the full thickness of SC (Figure 1c).

T. rubrum infection simultaneously altered integrity of the epidermal barrier and activated keratinocyte responses

The epidermal barrier integrity of RHE was assessed during infection by measurement of transepithelial electrical resistance and assessment of its permeability to Lucifer yellow fluorescent dye (Figure 2a–c). Sudden barrier alterations appeared on the fourth day following infection. Conversely, the barrier was strengthened over time in non-infected RHE. Additionally, inside-out permeability of RHE was studied using biotin dissolved in culture medium, revealing that the integrity of TJs was reduced on the fourth day after infection (Figure 2d). Accordingly, the TJ protein claudin-1 exhibited an altered distribution in infected RHE, as assessed by immunostaining (see Supplementary Figure S1 online).

Infection of RHE further triggered mRNA expression in keratinocytes, as well as the cells' release of cytokines (IL-8, IL-1α, IL-1β, TNFα, TSLP, and G-CSF), of protein TNFα-stimulated gene 6, and AMP (human β-defensin-2 [hBD2] and -3 [hBD3], S100A7) as revealed, respectively, by quantitative reverse transcriptase–PCR (RT-qPCR) and ELISA (Figure 2e and f and see Supplementary Figure S2 online). Conversely, except for transglutaminase-1, which was slightly overexpressed 1 day after infection, the expression of differentiation markers (filaggrin, involucrin, or loricrin) or of TLR2, TLR5, and TLR6 exhibited no alteration during infection (see Supplementary Figure S3 online). Expression and release of all factors studied remained unaltered inside RHE exposed either to phosphate buffered saline (PBS) alone or to heat-killed arthroconidia.

The copy number (CN) for the *DEFB4* gene, encoding hBD2, can range from 2 to 12 and is linked to variations in basal expression levels for hBD2 (Hollox et al., 2003). High CN in patients affords reduced susceptibility to dermatophytosis (Jaradat et al., 2015). The most frequent *DEFB4* CN in the population is 4, hence a CN of <4 is considered "low" and that of >4 as "high" (Jaradat et al., 2013). Eight primary keratinocyte cultures in our laboratory were genotyped to count *DEFB4* CN. Data revealed between 3 and 5 CN for this gene (see Supplementary Figure S4 online). Keratinocytes with 3 *DEFB4* CN were selected for RHE production in this study.

p38 MAPK inhibitor PD169316 hampers infection of RHE by affecting dermatophyte growth

Because activation of p38 MAPK has been associated with infection by dermatophytes (Achterman et al., 2015) and is also found in untreated RHE (Figure 3), a potential role for p38 MAPK during *T. rubrum* infection of RHE was investigated using the PD169316—a p38 MAPK-specific inhibitor. No further activation of p38 MAPK can be observed during RHE infection (Figure 3a). Thus, the actual inhibition of p38 MAPK activity by PD169316 was assessed through detection of phosphorylation of heat shock protein 27—considering that this is a known phosphorylation target of p38 MAPK in keratinocytes (Garmyn et al., 2001)—in RHE exposed to H_2O_2 in order to activate p38 MAPK signaling pathway (Peus et al., 1999; Mathay et al., 2008) (Figure 3b).

Interestingly, the presence of PD169316 prevents the epidermal barrier alterations that are usually induced on the fourth day after *T. rubrum* infection (Figure 4a–c). Furthermore, the extent of SC invasion by arthroconidia is also reduced (Figure 4d) whereas the overexpression of IL-8, IL-1α, IL-1β, TNFα, hBD2, and hBD3, usually induced by infection, is not observed in the presence of PD169316 (Figure 4e and see Supplementary Figure S5 online).

Because p38 MAPK activity seems unaltered during infection of RHE, a potential effect of PD169316 on *T. rubrum* growth itself was hypothesized and studied by seeding arthroconidia on Sabouraud agar (2% glucose and 1% peptone) containing PD169316. After a 7-day incubation

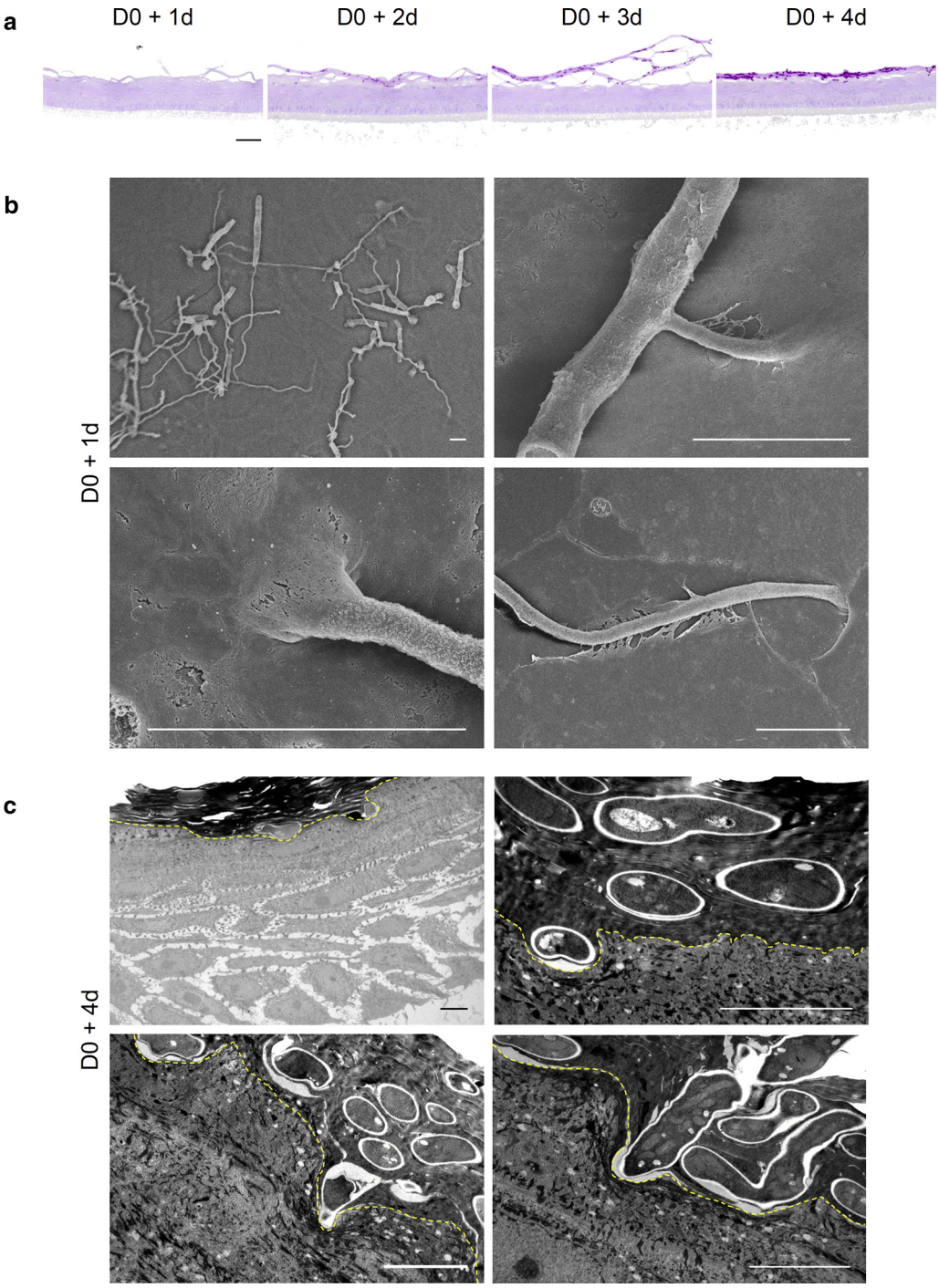

Figure 1. Fungal hyphae invade SC in RHE by progressing through intercellular space. (**a**) PAS staining with α-amylase treatment of histological sections prepared from RHE infected by *Trichophyton rubrum* arthroconidia for 1 (D0 + 1 day), 2 (D0 + 2 days), 3 (D0 + 3 days), or 4 (D0 + 4 days) days. Scale bar = 50 μm. (**b, c**) SC colonization and invasion of RHE by *T. rubrum* arthroconidia respectively assessed (**b**) by scanning electron microscopy performed 1 day after infection (D0 + 1 day) or (**c**) by transmission electron microscopy performed 4 days after infection (D0 + 4 days). Yellow dotted lines indicate limits between SC and *stratum granulosum*. Scale bars = 5 μm. PAS, periodic-acid Schiff; RHE, reconstructed human epidermis; SC, *stratum corneum*.

at 27 °C, the number of colony-forming units was reduced in the presence of PD169316, and colonies appeared smaller and more compact, while fungal hyphae seemed thinner and presented fewer septa when analyzed through scanning electron microscopy (Figure 5a and b). In good accordance with PD169316 having an effect on dermatophytes, the growth of *T. rubrum* arthroconidia on lyophilized RHE was impaired by PD169316 (Figure 5c). Similar growth inhibition was observed for two other species, *Trichophyton interdigitale* and *Trichophyton benhamiae*, seeded on Sabouraud agar containing PD169316 (Figure 5d and e). Conversely though, other p38 MAPK inhibitors, namely SB202190, SB203580, VX-702, and BIRB796, did not alter growth of *T. rubrum* (Figure 6), *T. interdigitale,* or *T. benhamiae* (see Supplementary Figure S6 online) on Sabouraud agar, nor the infection of RHE by *T. rubrum* arthroconidia (data not

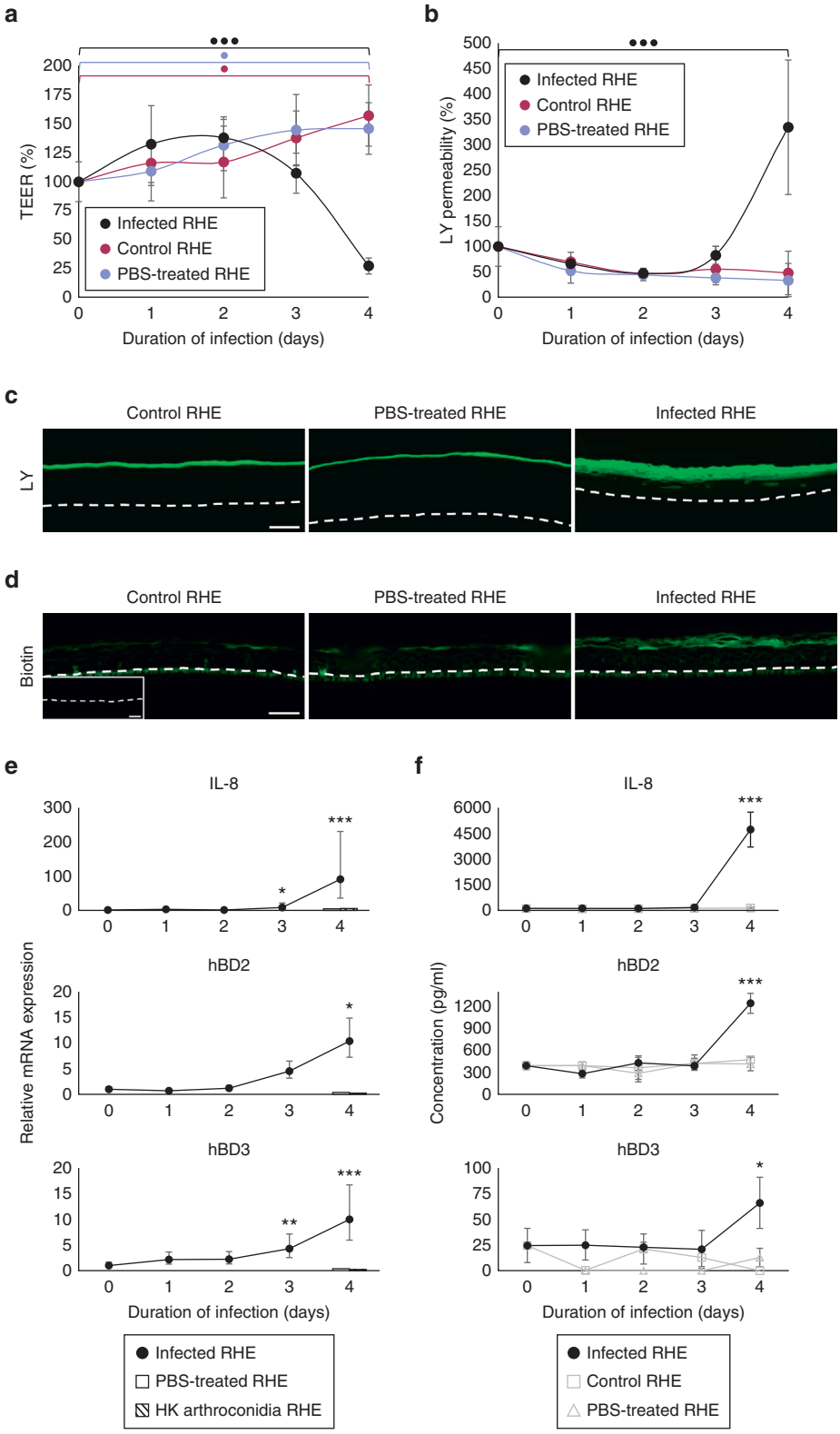

Figure 2. Infection of RHE by *Trichophyton rubrum* simultaneously induces epidermal barrier alterations and keratinocyte responses. (**a**) Transepithelial electrical resistance and (**b**) permeability to LY fluorescent dye of infected RHE compared with control and PBS-treated RHE (n = 6; mean ± standard deviation). (**c**) Fluorescence analysis of LY dye penetration in RHE and (**d**) localization of biotin by fluorescent-labeling after inside-out permeability assay on the fourth day after infection. Negative control incubated without biotin (inset); dotted lines show the filter. Scale bars = 50 μm. (**e**) Expression and (**f**) release of pro-inflammatory cytokine (IL-8) and AMP (hBD2, hBD3) by keratinocytes of infected RHE, compared with control and PBS-treated RHE and RHE exposed to HK arthroconidia, respectively assessed by RT-qPCR and ELISA in culture media (n = 3; mean ± confidence interval 95% or mean ± standard deviation for RT-qPCR or ELISA results, respectively). $*P < 0.05$, $**P < 0.01$, $***P < 0.001$, one-way ANOVA. ANOVA, analysis of variance; HK, heat-killed; LY, Lucifer yellow; PBS, phosphate buffered saline; RHE, reconstructed human epidermis; RT-qPCR, quantitative reverse transcriptase—PCR.

shown). Moreover, culture in presence of PD169316 or SB203580 did not suppress the growth of the fission yeast *Schizosaccharomyces pombe*, whereas strain knockout for *sty1*, the yeast homolog for p38 MAPK, exhibited drastically reduced cell growth under any culture condition (see Supplementary Figure S7 online).

DISCUSSION

The in vitro model of *T. rubrum* dermatophytosis in RHE has been previously validated as representative of in vivo human cutaneous dermatophytosis lesions (Faway et al., 2017). Here, we characterized the consequences of infection on epidermal barrier integrity, and the primary responses of keratinocytes.

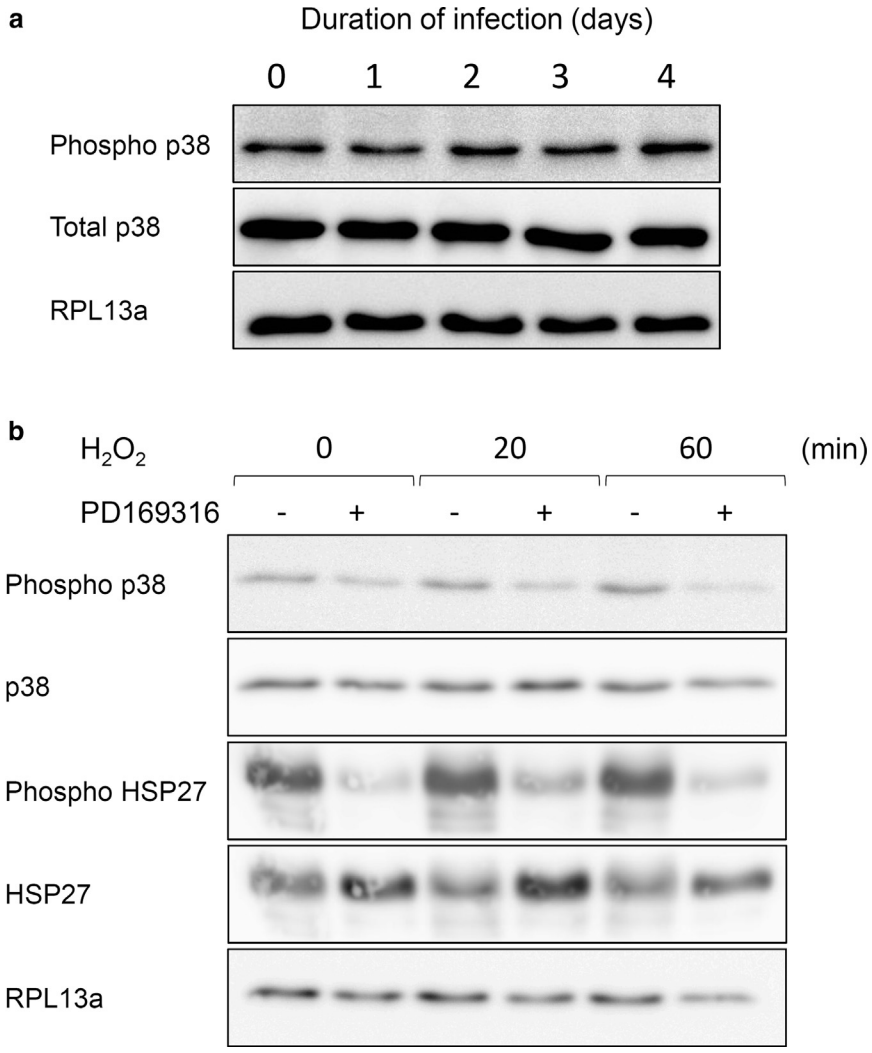

Figure 3. p38 MAPK is constitutively phosphorylated in RHE and its activity can be inhibited by PD169316. (**a**) Levels of p38 MAPK and phosphorylated p38 MAPK investigated by western blotting, using antibodies specific for p38 MAPK or phosphorylated p38 MAPK, after protein extraction from RHE, during *Trichophyton rubrum* infection (0 to 4 days). (**b**) Levels of p38 MAPK and phosphorylated p38 MAPK, as well as levels of HSP27 and phosphorylated HSP27 assessed by western blotting, using specific antibodies, on protein extracts from RHE, either previously treated for 24 hours with PD169316 (15 μM), a p38 MAPK-specific inhibitor, or not treated, then exposed to H_2O_2 (1 mM) for 20 or 60 minutes. The detection of RPL13a protein was used as loading control. HSP27, heat shock protein 27; MAPK, mitogen-activated protein kinase; RHE, reconstructed human epidermis.

Hyphae of *T. rubrum* invade SC and disrupt the epidermal barrier

Electron microscopy images suggest that *T. rubrum* hyphae invade the SC via intercellular progression between corneocytes. Furthermore, hyphae of *Trichophyton mentagrophytes* have previously been shown to invade the SC between corneocytes in both infected SC sheets (Aljabre et al., 1992) and skin sections (Duek et al., 2004). These results suggest that dermatophytes are able to orientate the direction of hyphal growth in relation to the physical and topographical features of the substrate, a phenomenon known as thigmotropism and regulated by complex molecular signaling pathways (Almeida and Brand, 2017). Thigmotropism is required in vitro and in vivo for invasion of host surfaces by pathogenic fungi, such as *C. albicans* and dermatophytes (Jayatilake et al., 2005; Perera et al., 1997; Piérard et al., 2007). These observations also suggest that dermatophytes may degrade corneodesmosomes and parts of the lipid extracellular matrix while hyphae invade the SC. As dermatophytes secrete several proteases during in vivo infection (Méhul et al., 2016; Tran et al., 2016), hyphae may thus be responsible for altering the barrier integrity observed during infection of RHE.

In the absence of an immune system and microbiome, the RHE barrier relies on physical components of SC and TJs (Proksch et al., 2008); this explains the observation that it strengthens over time in untreated RHE as a likely result of SC thickening. Barrier function of RHE that has been temporarily covered with PBS, increases similarly, suggesting that transient moistening of the epidermal surface does not alter barrier integrity. By contrast, the barrier of infected RHE is suddenly disrupted on the fourth day after infection by *T. rubrum* arthroconidia, in line with an observed increase of transepithelial water loss in biopsies from dermatophytosis cutaneous lesions (Jensen et al., 2007). In addition, the function of TJs is lost on the fourth day after RHE infection, concomitantly with the altered localization of claudin-1. Perturbed TJs have been reported as well in vitro and in vivo during *Staphylococcus aureus* infection, in association with simultaneous redistribution of TJ proteins (Bäsler et al., 2017; Ohnemus et al., 2008). Taken together, these observations suggest that invading hyphae progressively increase permeability of the SC. On the fourth day following infection, hyphae reaching the top of granular layer induce the alterations of TJs that correspond to the sudden loss in epidermal barrier

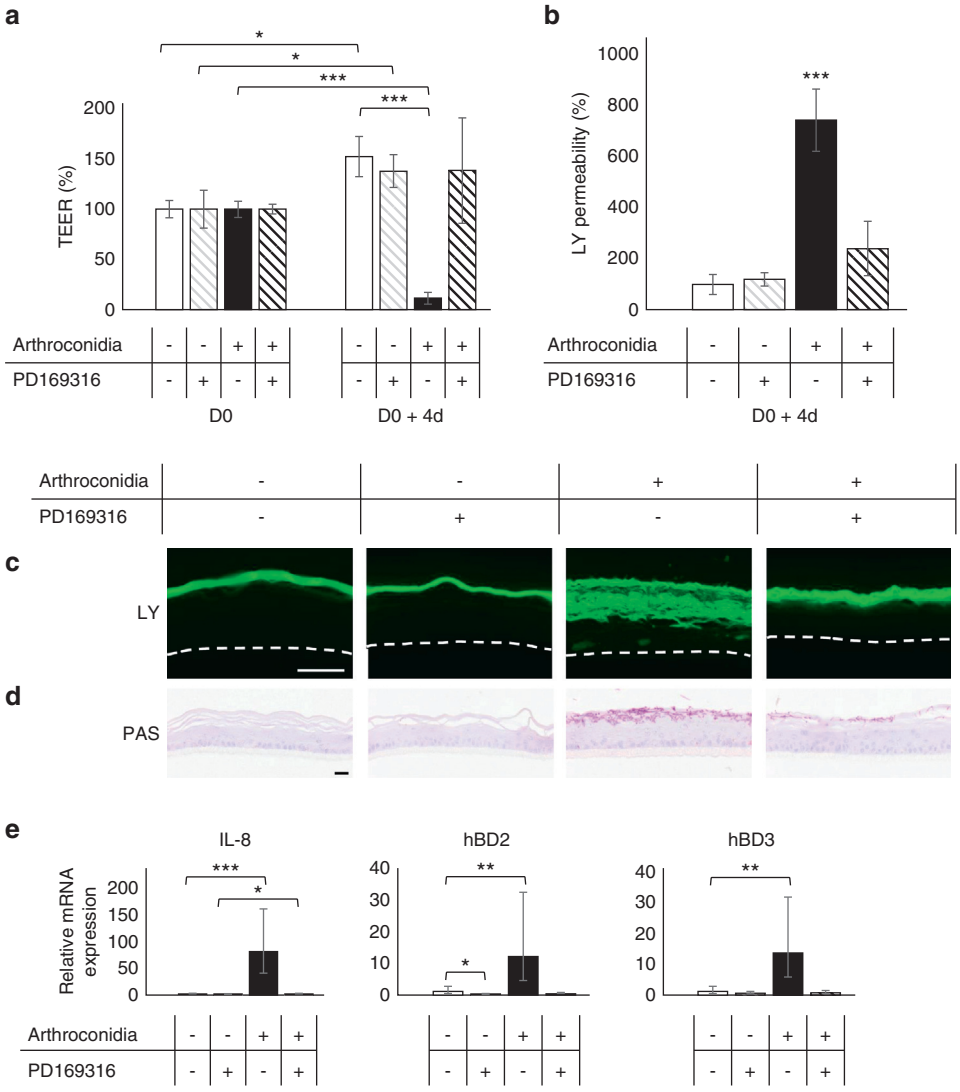

Figure 4. PD169316 hampers development of *Trichophyton rubrum* infection on RHE and prevents barrier alterations, as well as keratinocyte responses. RHE were cultured in presence or absence of PD169316 (15 μM) and either infected with *T. rubrum* arthroconidia for 4 days (D0 + 4 days) before barrier analysis and investigation of keratinocyte responses, or not infected. (**a**) Transepithelial electrical resistance and (**b**) permeability to LY fluorescent dye in four studied conditions (n = 3; mean ± standard deviation). (**c**) Analysis by fluorescent microscopy of LY dye penetration illustrated for the four conditions. Dotted lines localize the filter. Scale bar = 50 μm. (**d**) Same conditions observed by PAS staining with α-amylase pretreatment. Scale bar = 20 μm. (**e**) Relative mRNA expression of IL-8, hBD2, and hBD3 determined by RT-qPCR analysis of RNA extracts from RHE in same conditions (n = 3; mean ± confidence interval 95%). *$P < 0.05$, **$P < 0.01$, ***$P < 0.001$, one-way ANOVA. ANOVA, analysis of variance; LY, Lucifer yellow; PAS, periodic-acid Schiff; RHE, reconstructed human epidermis; RT-qPCR, quantitative reverse transcriptase–PCR.

integrity. In the absence of immune cells, this barrier disruption allows dermatophytes to colonize the full thickness of RHE. Further evidence is provided by histological demonstration that fungal elements invade living cell layers of RHE from the fifth day after infection (Faway et al., 2017). It is of note that mRNA expression of epidermal differentiation markers remains unaltered during *T. rubrum* infection of RHE, even though *T. rubrum* infection disturbs epidermal morphology. This observation does not exclude concomitant redistribution of differentiation markers, as previously observed in dermatophytosis lesions (Jensen et al., 2007).

T. rubrum infection induces inflammatory responses in RHE

Keratinocytes of infected RHE overexpress and release several cytokines (IL-1α, IL-1β, TNFα, IL-8) and AMP (hBD2, hBD3, S100A7) from the fourth day after infection. Release of G-CSF, an early response of epithelial cells to *Candida albicans* infection (Moyes et al., 2016), was detected at low concentration in our model, whereas IL-6 and RNase7 expression was scarcely detectable. In contrast, neither transient moistening of the tissue, nor exposure to killed arthroconidia induced those responses. Some in vitro studies report release of these cytokines by infected keratinocytes, while others do not (Achterman et al., 2015; Nakamura et al., 2002; Shiraki et al., 2006; Tani et al., 2007). Expression of pro-inflammatory cytokines and subsequent activation of T helper type 1 and T helper type 17 immunity have been observed in a mouse model of dermatophytosis (Cambier et al., 2014; Heinen et al., 2018). Furthermore, overexpression and release of hBD2, hBD3, RNase7, and S100A7 in response to dermatophytes have been demonstrated in vitro (Firat et al., 2014) and in vivo (Brasch et al., 2014). The apparent discrepancies in cytokine profiles may represent distinct keratinocyte responses to different dermatophytes species. In line with this, specific cytokine profiles characterize the responses to anthropophilic versus zoophilic dermatophytes species (Shiraki et al., 2006; Tani et al., 2007). In addition to inflammatory cytokines, TSG-6, an anti-inflammatory protein, was produced in response to *T. rubrum* infection of RHE. Accordingly, infection by *T. rubrum* induces the

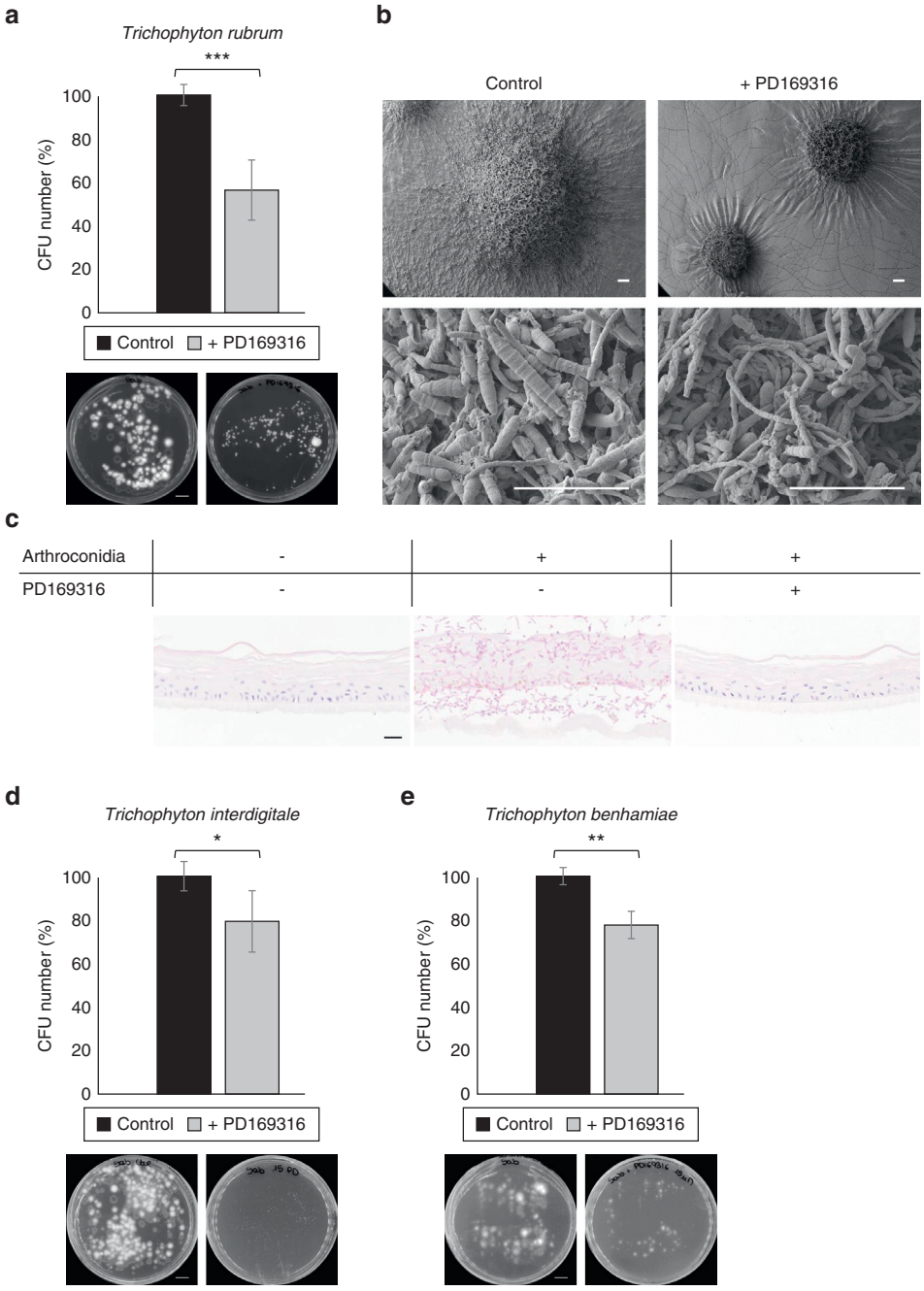

Figure 5. PD169316 impairs dermatophyte growth in culture on Sabouraud agar. Dermatophytes arthroconidia were seeded on Sabouraud agar containing PD169316 (15 μM) or lacking it (control) and incubated for 7 days at 27 °C. (**a**) Culture dishes illustrating colonies and comparison of *Trichophyton rubrum* growth determined by percentage of CFU versus control (n = 3; mean ± standard deviation). Scale bar = 1 cm. (**b**) Scanning electron microscopy observation of *T. rubrum* colonies. Lower panels present hyphae in colony centers at higher magnification. Scale bars = 100 μm. (**c**) PAS staining revealing infection by *T. rubrum* arthroconidia of lyophilized RHE and inhibition by PD169316. Scale bar = 20 μm. (**d, e**) Illustration of growth percentage determined by percentage of CFU versus control (n = 3; mean ± standard deviation) and macroscopic aspect of colonies obtained with *Trichophyton interdigitale* and *Trichophyton benhamiae*. Scale bars = 1 cm. *$P < 0.05$, **$P < 0.01$, ***$P < 0.001$, Student *t* test. CFU, colony-forming unit; PAS, periodic-acid Schiff; RHE, reconstructed human epidermis.

release of the anti-inflammatory cytokine IL-10 by macrophages (Campos et al., 2006).

The simultaneous activation of keratinocyte responses and epidermal barrier disruption suggests that both events are related. Perturbation of the epidermal barrier allows contact between dermatophytes and living granular keratinocytes that are able to recognize fungal molecular patterns through TLR (Netea et al., 2008), inducing production of cytokines and AMP. However, a reverse mechanism cannot be excluded: during invasion of SC by dermatophytes, granular keratinocytes could recognize fungal secreted material (Brouta et al., 2003; Descamps et al., 2003) and react by producing cytokines and AMP which can, in turn, influence the epidermal barrier (Kirschner et al., 2009).

PD169316 inhibits growth of dermatophytes

As p38 MAPK activation had been previously associated with dermatophyte infection (Achterman et al., 2015), its role during infection of RHE was monitored using PD169316, a p38 MAPK-specific inhibitor (Jans et al., 2004; Mathay et al., 2008). Unexpectedly, PD169316 was shown to inhibit growth of arthroconidia from *T. rubrum*, *T. interdigitale*, and *T. benhamiae*, both on RHE and on Sabouraud agar. Moreover, colonies grown in vitro in the

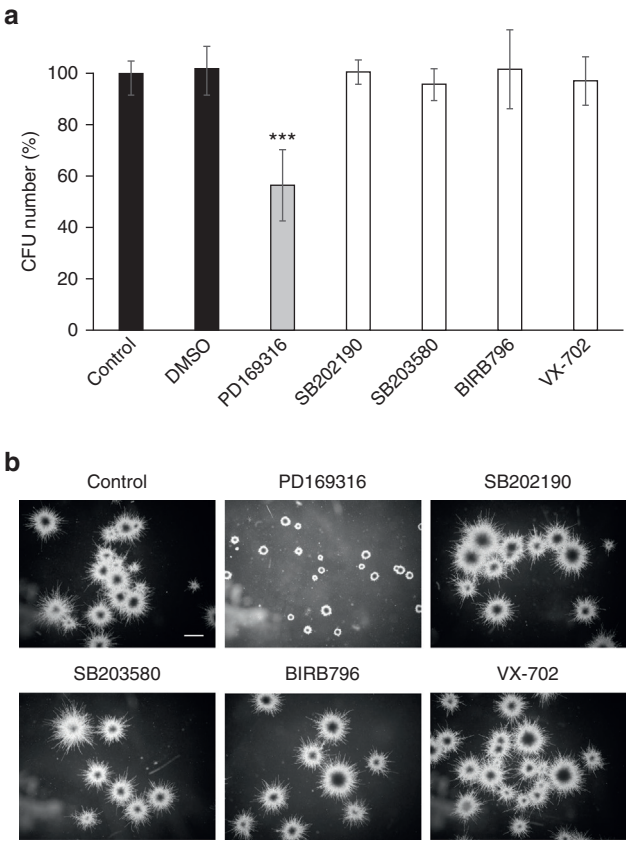

Figure 6. Among five well-known p38 MAPK inhibitors, PD169316 is the only one that alters dermatophytes growth. *Trichophyton rubrum* arthroconidia were seeded on Sabouraud agar containing 15 μM of different p38 MAPK-specific inhibitors and incubated for 7 days at 27 °C. (**a**) Growth percentage of *T. rubrum* evaluated by CFU counting (n = 3; mean ± standard deviation) and (**b**) by microscopic observations of colonies in the presence of the inhibitors. Scale bar = 1 mm. ***$P < 0.001$, Student *t* test. CFU, colony-forming unit; MAPK, mitogen-activated protein kinase.

presence of PD169316 are smaller and display abnormal morphology.

A candidate fungal target of PD169316 is a *T. rubrum* p38 protein kinase ortholog with 50% amino acid identity to human p38. However, PD169316 does not alter growth of yeast *S. pombe,* whose p38 MAPK ortholog (Sty1) shares 84% identity with *T. rubrum* p38 protein kinase. This observation suggests that the fungal target of PD169316, whose inhibition leads to dermatophytes growth impairment, could not be the p38 protein kinase. In addition, other p38 MAPK inhibitors SB202190, SB203580, VX-702, and BIRB796, do not inhibit dermatophyte growth on Sabouraud agar, nor infection of RHE. Thus, among the p38 MAPK inhibitors, PD169316 exhibits unique effects, as observed in a study investigating antiviral activities against Enterovirus71 (Zhang et al., 2017).

Summary

This report illustrates that *T. rubrum* infection of RHE results in simultaneous epidermal barrier disruption and activation of keratinocyte responses. It shows that PD169316 inhibits dermatophyte growth and thereby qualifies as a candidate drug against dermatophytosis.

MATERIALS AND METHODS

Dermatophyte strains, culture, and production of arthroconidia

The strains IHEM 13894 of *T. rubrum*, IHEM 00584 of *T. interdigitale,* and IHEM 20163 of *T. benhamiae*, isolated from naturally infected humans, were obtained from the Belgian Coordinated Collections of Microorganisms (BCCM/IHEM collection of biomedical fungi and yeasts, Brussels, Belgium). Arthroconidia were produced as previously described in Tabart et al. (2007). Briefly, dermatophytes grown at 27 °C on Sabouraud agar (containing 2% glucose and 1% peptone) were recovered and cultured on YEN agar (containing 2% yeast extract and 1% peptone) at 30 °C in an atmosphere containing 12% CO_2. The surface of the mycelium was scraped, added to sterile PBS, and this solution was stirred overnight at 4 °C and then filtered through three Miracloth layers (22−25 μm pore size; Millipore, Overijse, Belgium) to recover unicellular fungal elements corresponding to arthroconidia. Heat-killed arthroconidia were obtained by 10-minute incubation in a boiling water bath, followed by PBS washes.

Infection of RHE by *T. rubrum* dermatophyte

RHE was prepared as described (De Vuyst et al., 2014) and cultured in EpiLife medium (Cascade Biologics, Mansfield, UK), supplemented with Human Keratinocyte Growth Supplement (Cascade Biologics, Mansfield, UK) and containing 1.5 mM Ca^{2+}, 10 ng/ml keratinocyte growth factor (R&D system, Abingdon, UK), and 50 μg/ml vitamin C.

The procedure used for infection was previously described (Faway et al., 2017). Concisely, RHE was infected on day 0 (D0) by topical application of a PBS-suspension of *T. rubrum* arthroconidia, in order to reach a density of 1,700 arthroconidia per cm^2. Four hours later, the suspension was removed from RHE, followed by washes with PBS. Infected RHE was then cultured at 37 °C in a humidified atmosphere containing 5% CO_2 for 4 additional days with the culture medium renewed daily.

PBS-treated RHE consisted of RHE that only PBS was applied on D0 and that had undergone washes. For infection of RHE with heat-killed arthroconidia, PBS was first topically applied on D0, followed by washes four hours later. On the fourth day following PBS-exposure, 1,000,000 heat-killed *T. rubrum* arthroconidia were applied topically and infected RHE was finally analyzed, after four hours of incubation.

Histological analysis

For histological analysis, RHE was processed as described by De Vuyst et al. (2014). Periodic-acid Schiff staining was performed with hemalum counterstaining and pretreatment with α-amylase as previously described (Faway et al., 2017).

Assessment of epidermal barrier integrity

Transepithelial electrical resistance of RHE was measured using a Millicell ERS-2 Voltohmmeter (Millipore, Overijse, Belgium) and expressed as percentages of values determined in the RHE control.

To assess the permeability of RHE, 150 μl of fluorescent dye (Lucifer yellow vs. dilithium salt; Sigma-Aldrich, Munich, Germany) were laid on the surface of RHE placed over 200 μl of culture medium. RHE was incubated at 37 °C for 6 hours in a humidified atmosphere containing 5% CO_2. The amount of Lucifer yellow in the medium under the RHE was finally determined by measuring its fluorescence using a fluorescence reader. In addition, sections of

RHE were observed using a fluorescent microscope in order to localize Lucifer yellow in tissue.

To investigate efficiency of the inside-out barrier, we assessed biotin diffusion from culture media to the apical surface of RHE. After washes with PBS containing 1 mM $CaCl_2$, RHE was incubated at 37 °C in a humidified atmosphere containing 5% CO_2 for 30 minutes, over 500 µl of the same solution containing 2 mg/ml biotin (EZ-Link Sulfo-NHS-LC-Biotin; ThermoScientific, Rockford, IL). RHE was washed with PBS containing $CaCl_2$ and 100 mM glycine, fixed for 24 hours in 4% formaldehyde solution and, finally, embedded in paraffin. Tissue sections were stained with streptavidin conjugated to Alexa Fluor 488 (dilution 1:500; Invitrogen, Aalst, Belgium) and the localization of biotin was observed using a fluorescence microscope.

Immunostaining, electron microscopy, RNA extraction, RT-qPCR ELISA, and western blot

For detailed description of immunofluorescence staining of claudin-1, scanning and transmission electron microscopy, total RNA extraction, reverse-transcription and quantitative PCR, ELISA, and protein extraction and western blot analysis, see the Supplementary Materials and Methods.

p38 MAPK inhibitors

BIRB796 was purchased from Tocris (Abingdon, UK), PD169316 from Santa Cruz biotechnology (Heidelberg, Germany), SB202190 and SB203580 from InvivoGen (Toulouse, France), and VX-702 from Selleckchem (Munich, Germany). Concentration of each inhibitor was 15 µM.

In order to study the efficiency of PD169316, the p38 MAPK signaling pathway was stimulated by treating RHE for 20 or 60 minutes with 1 mM H_2O_2 added to the culture media, followed by one hour of recovery. PD169316 was present in culture media of RHE 24 hours before addition of H_2O_2 and during treatment and recovery.

Statistical analyses

All statistical analyses were carried out using SigmaPlot software, version 11.0. One-way analysis of variance and Student *t* test were performed to analyze the data.

DATA AVAILABILITY STATEMENT

Datasets related to this article available at https://doi.org/10.17632/srfzmgmcg4.1, an open-source online data repository hosted at Mendeley Data.

ORCIDs

Emilie Faway: http://orcid.org/0000-0003-3406-1103
Ludivine Cambier: http://orcid.org/0000-0001-8666-1317
Evelyne De Vuyst: http://orcid.org/0000-0001-7152-1370
Céline Evrard: http://orcid.org/0000-0002-7450-0759
Marc Thiry: http://orcid.org/ 0000-0001-7736-8709
Catherine Lambert de Rouvroit: https://orcid.org/0000-0002-0273-8995
Bernard Mignon: http://orcid.org/0000-0002-5958-4325
Yves Poumay: http://orcid.org/0000-0001-5200-3367

CONFLICT OF INTEREST

The authors state no conflict of interest.

ACKNOWLEDGMENTS

The authors gratefully acknowledge the technical help provided by B Balau, C Charlier, V De Glas, C De Mazy, K De Swert, J Gilloteaux, V Migeot, P Piscicelli, and D Van Vlaender. Correction of English by V Welch is gratefully acknowledged. Special thanks to B Bienfait and JS Blairvacq for providing skin samples, and to D Hermand for providing *S. pombe* strains. Funding for this research was obtained from the Région Wallonne (MYCAVERT, convention/grant id 1318058).

AUTHOR CONTRIBUTIONS

Conceptualization: EF, LC, CLDR, BM, YP; Formal Analysis: EF; Funding Acquisition: LC, CLDR, BM, YP; Investigation: EF, LC, CE, MT; Methodology: EF, LC, EDV, CLDR, BM, YP; Project Administration: EF, LC, CLDR, BM, YP; Validation: EF, CLDR, BM, YP; Visualization: EF, CLDR, BM, YP; Writing - Review and Editing: EF, CLDR, BM, YP

SUPPLEMENTARY MATERIAL

Supplementary material is linked to the online version of the paper at www.jidonline.org, and at 10.1016/j.jid.2019.03.1147.

REFERENCES

Achterman RR, Moyes DL, Thavaraj S, Smith AR, Blair KM, White TC, et al. Dermatophytes activate skin keratinocytes via mitogen-activated protein kinase signaling and induce immune responses. Infect Immun 2015;83:1705–14.

Aljabre SH, Richardson MD, Scott EM, Shankland GS. Germination of *Trichophyton mentagrophytes* on human stratum corneum *in vitro*. J Med Vet Mycol 1992;30:145–52.

Almeida MC, Brand AC. Thigmo responses: the fungal sense of touch. Microbiol Spectr 2017;5:FUNK-0040–2016.

Baldo A, Mathy A, Tabart J, Camponova P, Vermout S, Massart L, et al. Secreted subtilisin Sub3 from *Microsporum canis* is required for adherence to but not for invasion of the epidermis. Br J Dermatol 2010;162:990–7.

Bäsler K, Bergmann S, Heisig M, Naegel A, Zorn-Kruppa M, Brandner JM. The role of tight junctions in skin barrier function and dermal absorption. J Control Release 2016;242:105–18.

Bäsler K, Galliano MF, Bergmann S, Rohde H, Wladykowski E, Vidal-y-Sy S, et al. Biphasic influence of *Staphylococcus aureus* on human epidermal tight junctions. Ann N Y Acad Sci 2017;1405:53–70.

Brandner JM. Importance of tight junctions in relation to skin barrier function. Curr Probl Dermatol 2016;49:27–37.

Brasch J, Mörig A, Neumann B, Proksch E. Expression of antimicrobial peptides and toll-like receptors is increased in *tinea* and *pityriasis versicolor*. Mycoses 2014;57:147–52.

Brouta F, Descamps F, Vermout S, Monod M, Losson B, Mignon B. Humoral and cellular immune response to a *Microsporum canis* recombinant keratinolytic metalloprotease (r-MEP3) in experimentally infected guinea pigs. Med Mycol 2003;41:495–501.

Burstein VL, Guasconi L, Beccacece I, Theumer MG, Mena C, Prinz I, et al. IL-17-mediated immunity controls skin infection and T helper 1 response during experimental *Microsporum canis* dermatophytosis. J Invest Dermatol 2018;138:1744–53.

Calderon RA, Hay RJ. Cell-mediated immunity in experimental murine dermatophytosis. II. Adoptive transfer of immunity to dermatophyte infection by lymphoid cells from donors with acute or chronic infections. Immunology 1984;53:465–72.

Cambier L, Weatherspoon A, Defaweux V, Bagut ET, Heinen MP, Antoine N, et al. Assessment of the cutaneous immune response during *Arthroderma benhamiae* and *A. vanbreuseghemii* infection using an experimental mouse model. Br J Dermatol 2014;170:625–33.

Cambier LC, Heinen MP, Bagut ET, Antoine NA, Mignon BR. Overexpression of TLR-2 and TLR-4 mRNA in feline polymorphonuclear neutrophils exposed to *Microsporum canis*. Vet Dermatol 2016;27:78–81e22.

Campos MR, Russo M, Gomes E, Almeida SR. Stimulation, inhibition and death of macrophages infected with *Trichophyton rubrum*. Microbes Infect 2006;8:372–9.

De Vuyst E, Charlier C, Giltaire S, De Glas V, de Rouvroit CL, Poumay Y. Reconstruction of normal and pathological human epidermis on polycarbonate filter. Methods Mol Biol 2014;1195:191–201.

Descamps F, Brouta F, Vermout S, Monod M, Losson B, Mignon B. Recombinant expression and antigenic properties of a 31.5-kDa keratinolytic subtilisin-like serine protease from *Microsporum canis*. FEMS Immunol Med Microbiol 2003;38:29–34.

Duek L, Kaufman G, Ulman Y, Berdicevsky I. The pathogenesis of dermatophyte infections in human skin sections. J Infect 2004;48:175–80.

Faway É, Cambier L, Mignon B, Poumay Y, Lambert de Rouvroit C. Modeling dermatophytosis in reconstructed human epidermis: a new tool to study

infection mechanisms and to test antifungal agents. Med Mycol 2017;55:485–94.

Firat YH, Simanski M, Rademacher F, Schröder L, Brasch J, Harder J. Infection of keratinocytes with *Trichophyton rubrum* induces epidermal growth factor-dependent RNase 7 and human beta-defensin-3 expression. PLOS ONE 2014;9:e93941.

García-Madrid L, Huizar-López M, Flores-Romo L, Islas-Rodríguez A. *Trichophyton rubrum* manipulates the innate immune functions of human keratinocytes. Cent Eur J Biol 2011;6:902–10.

Garmyn M, Mammone T, Pupe A, Gan D, Declercq L, Maes D. Human keratinocytes respond to osmotic stress by p38 MAP kinase regulated induction of HSP70 and HSP27. J Invest Dermatol 2001;117:1290–5.

Haftek M. Epidermal barrier disorders and corneodesmosome defects. Cell Tissue Res 2015;360:483–90.

Havlickova B, Czaika VA, Friedrich M. Epidemiological trends in skin mycoses worldwide. Mycoses 2008;51:2–15.

Hayette M, Sacheli R. Dermatophytosis, trends in epidemiology and diagnostic approach. Curr Fungal Infect Rep 2015;9:164–79.

Heinen MP, Cambier L, Antoine N, Gabriel A, Gillet L, Bureau F, et al. Th1 and Th17 immune responses act complementary to optimally control superficial dermatophytosis. J Investig Dermatol 2018;139:626–37.

Hollox EJ, Armour JA, Barber JC. Extensive normal copy number variation of a β–defensin antimicrobial-gene cluster. Am J Hum Genet 2003;73:591–600.

Jans R, Atanasova G, Jadot M, Poumay Y. Cholesterol depletion upregulates involucrin expression in epidermal keratinocytes through activation of p38. J Invest Dermatol 2004;123:564–73.

Jaradat SW, Cubillos S, Krieg N, Lehmann K, Issa B, Piehler S, et al. Low DEFB4 copy number and high systemic hBD-2 and IL-22 levels are associated with dermatophytosis. J Invest Dermatol 2015;135:750–8.

Jaradat SW, Hoder-Przyrembel C, Cubillos S, Krieg N, Lehmann K, Piehler S, et al. Beta-defensin-2 genomic copy number variation and chronic periodontitis. J Dent Res 2013;92:1035–40.

Jayatilake JA, Samaranayake YH, Samanarayake LP. An ultrastructural and a cytochemical study of candida invasion of reconstituted human oral epithelium. J Oral Pathol Med 2005;34:240–6.

Jensen JM, Pfeiffer S, Akaki T, Schröder JM, Kleine M, Neumann C, et al. Barrier function, epidermal differentiation, and human β-defensin 2 expression in *Tinea corporis*. J Invest Dermatol 2007;127:1720–7.

Kirschner N, Poetzl C, von den Driesch P, Wladykowski E, Moll I, Behne MJ, et al. Alteration of tight junction proteins is an early event in psoriasis: putative involvement of proinflammatory cytokines. Am J Pathol 2009;175:1095–106.

Kirschner N, Rosenthal R, Furuse M, Moll I, Fromm M, Brandner JM. Contribution of tight junction proteins to ion, macromolecule, and water barrier in keratinocytes. J Invest Dermatol 2013;133:1161–9.

Kyriakis JM, Avruch J. Mammalian MAPK signal transduction pathways activated by stress and inflammation: a 10-year update. Physiol Rev 2012;92:689–737.

Lee WJ, Kim SL, Jang YH, Lee SJ, Kim DW, Bang YJ, et al. Increasing prevalence of *Trichophyton rubrum* identified through an analysis of 115,846 cases over the last 37 years. J Korean Med Sci 2015;30:639–43.

Li M, Chen Q, Tang R, Shen Y, Liu WD. The expression of β-defensin-2, 3 and LL-37 induced by *Candida albicans* phospholipomannan in human keratinocytes. J Dermatol Sci 2011;61:72–5.

Martinez-Rossi NM, Peres NT, Rossi A. Pathogenesis of dermatophytosis: sensing the host tissue. Mycopathologia 2017;182:215–27.

Mathay C, Giltaire S, Minner F, Bera E, Hérin M, Poumay Y. Heparin-binding EGF-like growth factor is induced by disruption of lipid rafts and oxidative stress in keratinocytes and participates in the epidermal response to cutaneous wounds. J Invest Dermatol 2008;128:717–27.

Méhul B, Gu Z, Jomard A, Laffet G, Feuilhade M, Monod M. (Tri r 2), an onychomycosis marker revealed by proteomics analysis of *Trichophyton rubrum* secreted proteins in patient nail samples. J Investig Dermatol 2016;136:331–3.

Mignon B, Tabart J, Baldo A, Mathy A, Losson B, Vermout S. Immunization and dermatophytes. Curr Opin Infect Dis 2008;21:134–40.

Moyes DL, Wilson D, Richardson JP, Mogavero S, Tang SX, Wernecke J, et al. Candidalysin is a fungal peptide toxin critical for mucosal infection. Nature 2016;532:64–8.

Nakamura Y, Kano R, Hasegawa A, Watanabe S. Interleukin-8 and tumor necrosis factor alpha production in human epidermal keratinocytes induced by *Trichophyton mentagrophytes*. Clin Diagn Lab Immunol 2002;9:935–7.

Netea MG, Brown GD, Kullberg BJ, Gow NA. An integrated model of the recognition of *Candida albicans* by the innate immune system. Nat Rev Microbiol 2008;6:67–78.

Ohnemus U, Kohrmeyer K, Houdek P, Rohde H, Wladykowski E, Vidal S, et al. Regulation of epidermal tight-junctions (TJ) during infection with exfoliative toxin-negative *Staphylococcus* strains. J Investig Dermatol 2008;128:906–16.

Perera TH, Gregory DW, Marshall D, Gow NA. Contact-sensing by hyphae of dermatophytic and saprophytic fungi. J Med Vet Mycol 1997;35:289–93.

Peus D, Vasa RA, Beyerle A, Meves A, Krautmacher C, Pittelkow MR. UVB activates ERK1/2 and p38 signaling pathways via reactive oxygen species in cultured keratinocytes. J Invest Dermatol 1999;112:751–6.

Piérard GE, Piérard-Franchimont C, Quatresooz P. Fungal thigmotropism in onychomycosis and in a clear hydrogel pad model. Dermatology 2007;215:107–13.

Proksch E, Brandner JM, Jensen JM. The skin: an indispensable barrier. Exp Dermatol 2008;17:1063–72.

Seebacher C, Bouchara JP, Mignon B. Updates on the epidemiology of dermatophyte infections. Mycopathologia 2008;166:335–52.

Shiraki Y, Ishibashi Y, Hiruma M, Nishikawa A, Ikeda S. Cytokine secretion profiles of human keratinocytes during *Trichophyton tonsurans* and *Arthroderma benhamiae* infections. J Med Microbiol 2006;55:1175–85.

Tabart J, Baldo A, Vermout S, Nusgens B, Lapiere C, Losson B, et al. Reconstructed interfollicular feline epidermis as a model for *Microsporum canis* dermatophytosis. J Med Microbiol 2007;56:971–5.

Tani K, Adachi M, Nakamura Y, Kano R, Makimura K, Hasegawa A, et al. The effect of dermatophytes on cytokine production by human keratinocytes. Arch Dermatol Res 2007;299:381–7.

Tran VDT, De Coi N, Feuermann M, Schmid-Siegert E, Băguț ET, Mignon B, et al. RNA sequencing-based genome reannotation of the dermatophyte *Arthroderma benhamiae* and characterization of its secretome and whole gene expression profile during infection. mSystems 2016;1:00036–16.

van Smeden J, Bouwstra JA. Stratum corneum lipids: their role for the skin barrier function in healthy subjects and atopic dermatitis patients. Curr Probl Dermatol 2016;49:8–26.

Vermout S, Tabart J, Baldo A, Mathy A, Losson B, Mignon B. Pathogenesis of dermatophytosis. Mycopathologia 2008;166:267–75.

Weitzman I, Summerbell RC. The dermatophytes. Clin Microbiol Rev 1995;8:240–59.

Zarubin T, Han J. Activation and signaling of the p38 MAP kinase pathway. Cell Res 2005;15:11–8.

Zhan P, Liu W. The changing face of dermatophytic infections worldwide. Mycopathologia 2017;182:77–86.

Zhang Z, Wang B, Wu S, Wen Y, Wang X, Song X, et al. PD169316, a specific p38 inhibitor, shows antiviral activity against Enterovirus71. Virology 2017;508:150–8.

SUPPLEMENTARY MATERIALS AND METHODS

Claudin-1 immunostaining

For immunostaining of claudin-1, tissue sections were incubated in 10 mM citrate buffer pH 6 at 100 °C for 20 minutes. After slow cooling at room temperature, sections were immersed in phosphate buffered saline (PBS) containing 0.1 M glycine. Blocking was performed in PBS containing 0.2% BSA for 30 minutes, before overnight incubation at 4 °C with rabbit polyclonal anti–claudin-1 antibody (dilution 1:50; Invitrogen, Aalst, Belgium). Sections were then incubated for 45 minutes with goat anti-rabbit IgG H&L (Alexa Fluor 488; dilution 1:1000; Abcam, Cambridge, UK). Finally, coverslips were mounted in Mowiol and tissue sections were observed using confocal microscopy. Negative control was obtained by incubation overnight at 4 °C in PBS–BSA, instead of the solution containing the primary antibody.

Scanning and transmission electron microscopy

To observe *Trichophyton rubrum* colonies over Sabouraud agar by scanning electron microscopy, an agar surface of approximately 1 cm^2 was seeded. Infected reconstructed human epidermis (RHE) was analyzed after 24 hours of culture. All samples were fixed for 4 hours with 2.5% glutaraldehyde in 0.1 M sodium cacodylate buffer pH 7.4 at 4 °C. Then, they were rinsed three times with 0.2 M sodium cacodylate buffer pH 7.4 and dehydrated with increasing ethanol concentration (30–100%). After critical-point drying for infected RHE, or Hexamethyldisilazane drying for colonies over Sabouraud agar, and gold-coating, samples were analyzed using JSM-7500F scanning electron microscope (JEOL, Tokyo, Japan) at 5 kV.

For observation by transmission electron microscopy, control and infected RHE were fixed at 4 °C for 1 hour with 2.5% glutaraldehyde in 0.1 M Sörensen's buffer, rinsed three times with this buffer, and postfixed for 1 hour with 2% OsO_4 in the same buffer. After three washes in distilled water, samples were dehydrated in ascending concentrations of ethanol (70–100%) and embedded in Epoxy resin. Finally, ultrathin sections were contrasted with uranyl acetate and lead citrate and observed using JEM-1400 transmission electron microscope (JEOL) at 80 kV.

RNA extraction, reverse-transcription, and quantitative PCR analysis

Total RNA was extracted from infected and control (i.e., PBS-treated RHE and RHE exposed to heat-killed arthroconidia) RHE using RNeasy Mini Kit (Qiagen, Hilden, Germany) according to the manufacturer's instructions. Concentration and purity of extracted RNA were determined using a NanoDrop 1000 Spectrophotometer (Thermo Scientific, Rockford, IL). Subsequently, RNA was reverse-transcribed into cDNA using the SuperScript III Reverse Transcriptase kit (Invitrogen, Aalst, Belgium). The cDNA was diluted 1:20 in distilled water and stored at −20 °C.

All primers used for QPCR showed an efficacy between 85% and 110% and are described in Supplementary Table S1 (online). The QPCR mixture was composed of Takyon ROX SYBR Master Mix (Eurogentec, Seraing, Belgium), 300 nM of each primer and 5 µl of cDNA 1:20 in a total volume of 20 µl. The amplification protocol started with a 10-minute denaturation at 95 °C, followed by 45 cycles of denaturation for 10 seconds at 95 °C, annealing for 10 seconds at 60 °C, and elongation for 10 seconds at 72 °C, and was performed using Light Cycler 96 (Roche, Basel, Switzerland). *RPLP0* was used as reference gene.

ELISA

To assess the release of cytokines or antimicrobial peptides by keratinocytes, ELISA was performed on culture media using the commercial ELISA kits listed in Supplementary Table S2 (online).

Protein extraction and western blotting

Proteins were extracted from RHE via 5-minute incubation in twice-concentrated Laemmli buffer (62.5 mM Tris-HCl, 2% SDS, 8.7% glycerol, 0.05% bromophenol blue, 0.2% dithiothreitol) in a boiling water bath. Then, proteins were analyzed by sodium dodecyl sulfate–polyacrylamide gel electrophoresis and transferred onto polyvinylidene difluoride membrane (ThermoScientific, Rockford, IL). Blocking of the membrane in PBS containing 1% Tween 20 and 5% powdered milk was followed by overnight incubation at 4 °C with primary antibody. After washes, the membrane was incubated for one hour at room temperature with horseradish peroxidase-conjugated secondary antibody before chemiluminescent detection performed using BM Chemiluminescence Blotting Substrate (Roche Diagnostics, Mannheim, Germany). The detection of RPL13a protein was used as a loading control. Primary antibodies used for western blotting are described in Supplementary Table S3 (online).

DEFB4 gene copy number

Genomic DNA was extracted from keratinocytes using the DNeasy Blood and Tissue Kit (Qiagen, Hilden, Germany) according to the manufacturer's instructions. Genomic DNA was then subjected to a quantitative PCR amplification, using the TaqMan Copy Number Assays (Applied Biosystems, Lennik, Belgium) and copy number of the *DEFB4* gene was determined in relation to a reference DNA with known copy number of the *DEFB4* gene (DNA C0913, Culture Collections from Public Health England, UK).

Schizosaccharomyces pombe growth assay

Wild-type (#94 h-) and *sty1* knockout (#903 h- *sty1::kanR*) strains of *S. pombe* were grown in liquid YES medium at 37 °C overnight. The optical density at 595 nm was measured and cultures were diluted to optical density 0.05 (corresponding to 5.5×10^5 cells/ml) and divided into control and treated conditions (0.1% DMSO, 15 µM PD169316, 15 µM SB203580). The different cultures were then grown at 37 °C in YES medium for 24 hours; DMSO, PD169316, or SB203580 being added in culture suspension after two hours. Growth was monitored over time by measuring the optical density at 595 nm 0, 2, 4, 6, 10, and 24 hours after the culture began.

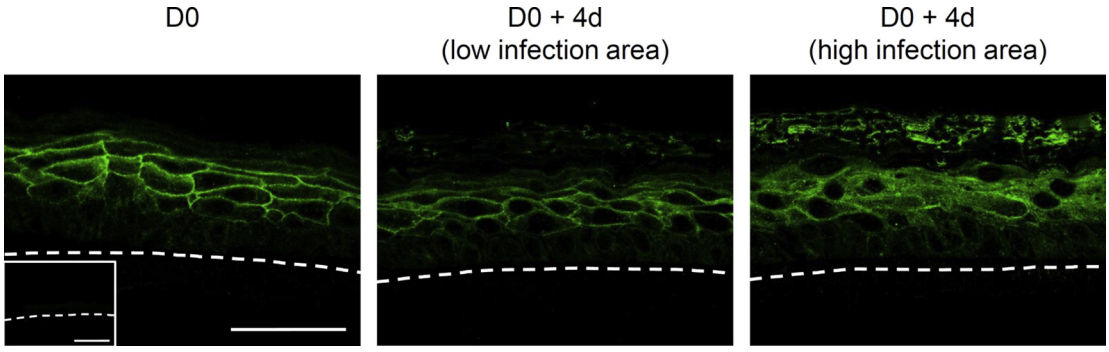

Supplementary Figure S1. Cldn-1 relocalizes in keratinocytes during infection of RHE by *Trichophyton rubrum* arthroconidia. Immunofluorescence localization of Cldn-1 before (D0) and after 4 days of infection (D0 + 4 days), either in low or in high infection area. Some cross-reaction between the antibody to Cldn-1 and *T. rubrum* arthroconidia can be noticed. Control staining without primary antibody (inset); dotted lines indicate localization of the filter. Scale bars = 50 μm. Cldn-1, claudin-1; RHE, reconstructed human epidermis.

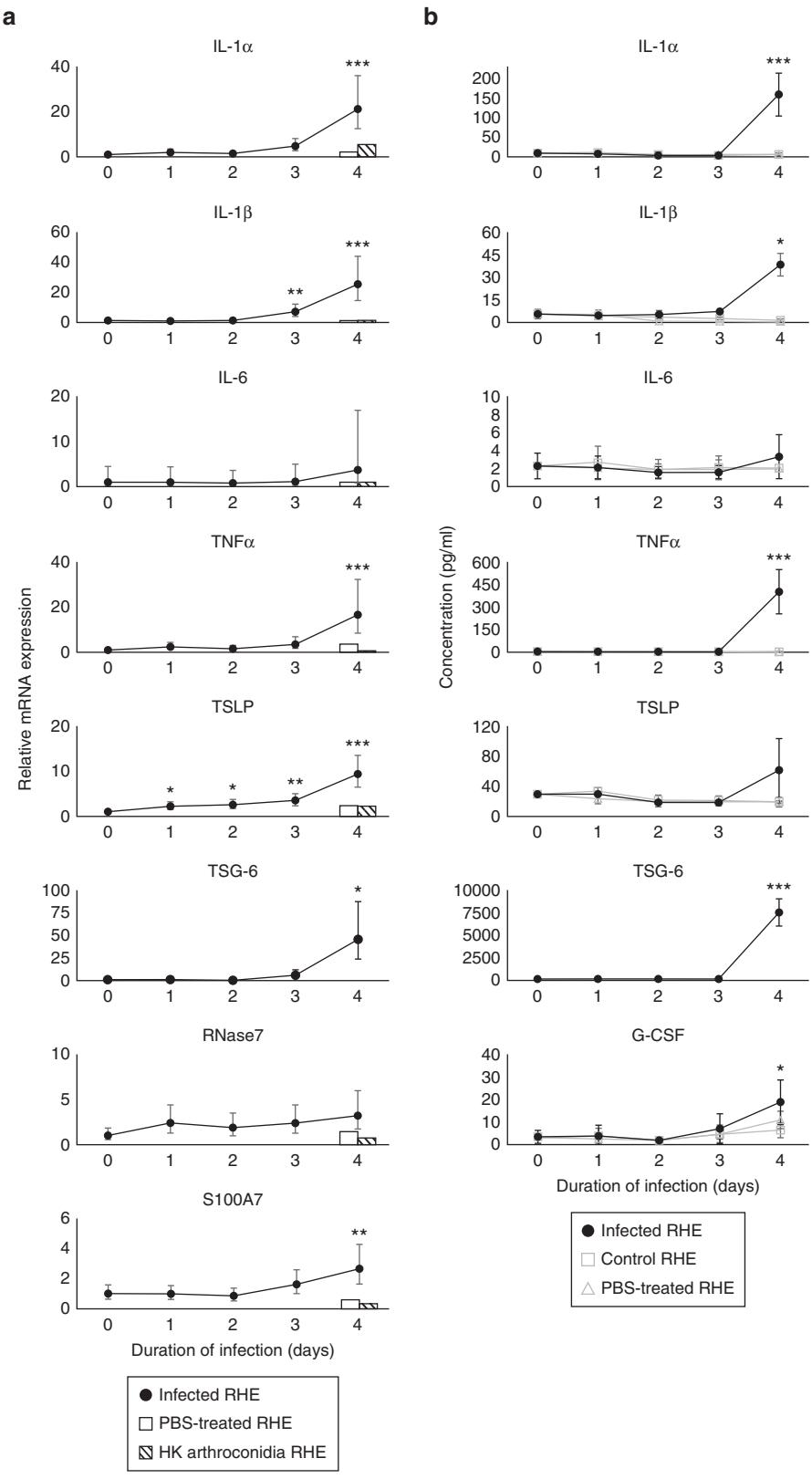

Supplementary Figure S2. Inflammatory cytokines, TSG-6 protein, and (AMP) are overexpressed and released by keratinocytes during *Trichophyton rubrum* infection. (**a**) Expression and (**b**) release of inflammatory cytokines (IL-1α, IL-1β, IL-6, TNFα, TSLP, G-CSF), TSG-6 protein, and AMP (RNase7, S100A7) by keratinocytes inside infected RHE compared with those parameters determined in control RHE, and in RHE exposed to PBS only or to HK arthroconidia. Expression was evaluated by RT-qPCR after RNA extraction from control and infected RHE (n = 3; mean ± confidence interval 95%) and cell release was measured by ELISA assay on culture media (n = 3; mean ± standard deviation). *$P < 0.05$, **$P < 0.01$, ***$P < 0.001$, compared with D0, one-way ANOVA. AMP, antimicrobial peptides; ANOVA, analysis of variance; HK, heat-killed; PBS, phosphate buffered saline; RHE, reconstructed human epidermis; RT-qPCR, quantitative reverse transcriptase—PCR.

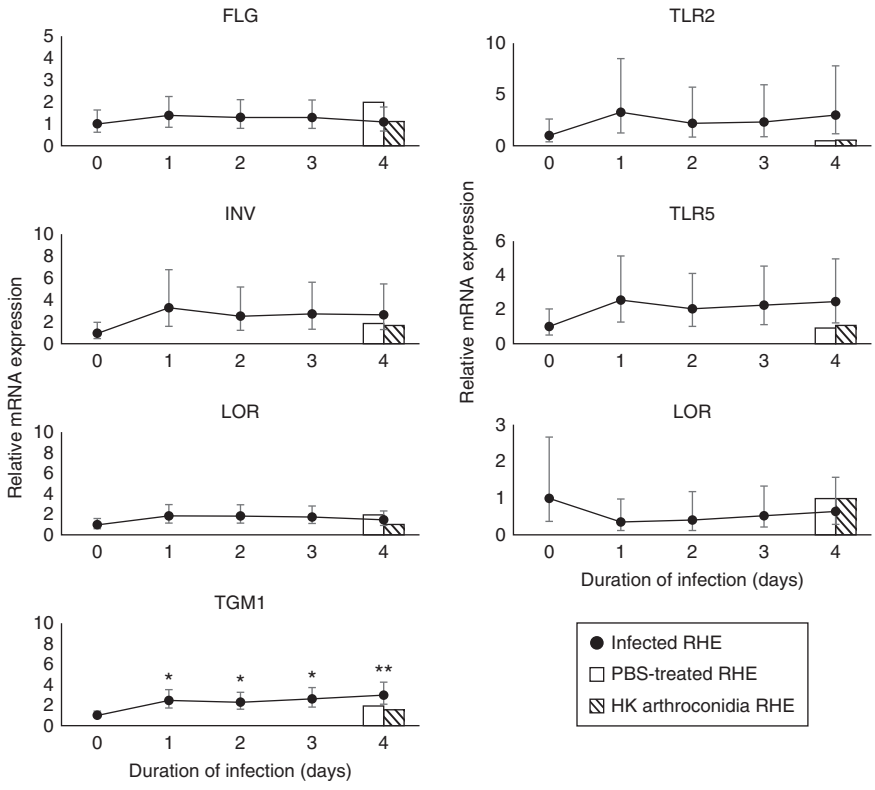

Supplementary Figure S3. TGM1 is overexpressed by keratinocytes during *Trichophyton rubrum* infection. Relative mRNA expression of differentiation markers, FLG, IVL, LOR, and TGM1, or TLR2, TLR5, and TLR6 in infected RHE in comparison with RHE exposed to PBS only or to heat-killed arthroconidia (n = 3; mean ± confidence interval 95%). *$P < 0.05$, **$P < 0.01$, compared with D0, one-way ANOVA. ANOVA, analysis of variance; FLG, filaggrin; IVL, involucrin; LOR, loricrin; PBS, phosphate buffered saline; RHE, reconstructed human epidermis; TGM1, transglutaminase-1; TLR, toll-like receptor.

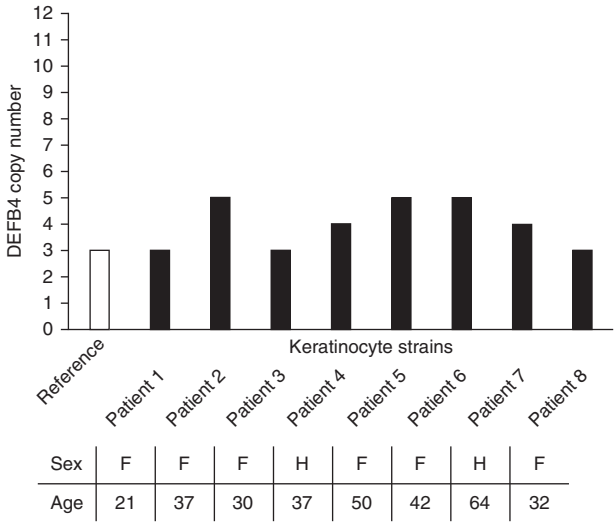

Sex	F	F	F	H	F	F	H	F
Age	21	37	30	37	50	42	64	32

Supplementary Figure S4. Copy number of *DEFB4* gene, encoding antimicrobial peptide hBD2, in strains of primary keratinocytes used to produce RHE. *DEFB4* gene CN assessed by quantitative PCR after genomic DNA extraction from primary keratinocytes cultured from eight patients. The most frequent *DEFB4* CN in the population is 4; CN <4 is considered low while those >4 are considered high CN. Investigations reveal between three and five copies of this gene in available strains. Primary keratinocytes cultured from patients 3 and 8, characterized by low *DEFB4* CN, were selected to produce RHE in our study. CN, copy number; RHE, reconstructed human epidermis.

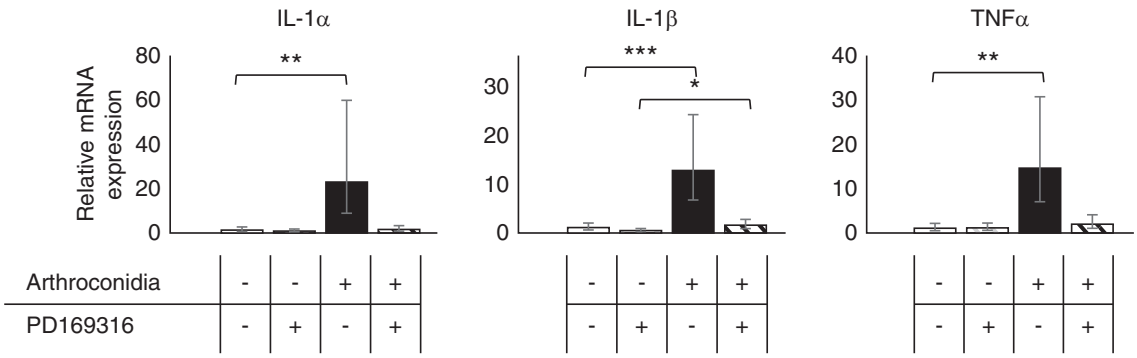

Supplementary Figure S5. PD169316 hampers the expression of inflammatory cytokines IL-1α, IL-1β, and TNFα by keratinocytes during *Trichophyton rubrum* infection. RHE was cultured in presence or not of PD169316 (15 μM) in medium and analyzed on the fourth day following infection (D0 + 4 days). Relative mRNA expression of inflammatory cytokines was measured by RT-qPCR after RNA extraction (n = 3; mean ± confidence interval 95%). *$P < 0.05$, **$P < 0.01$, ***$P < 0.001$, one-way ANOVA. ANOVA, analysis of variance; RHE, reconstructed human epidermis; RT-qPCR, quantitative reverse transcriptase–PCR; TNFα, tumor necrosis factor-α.

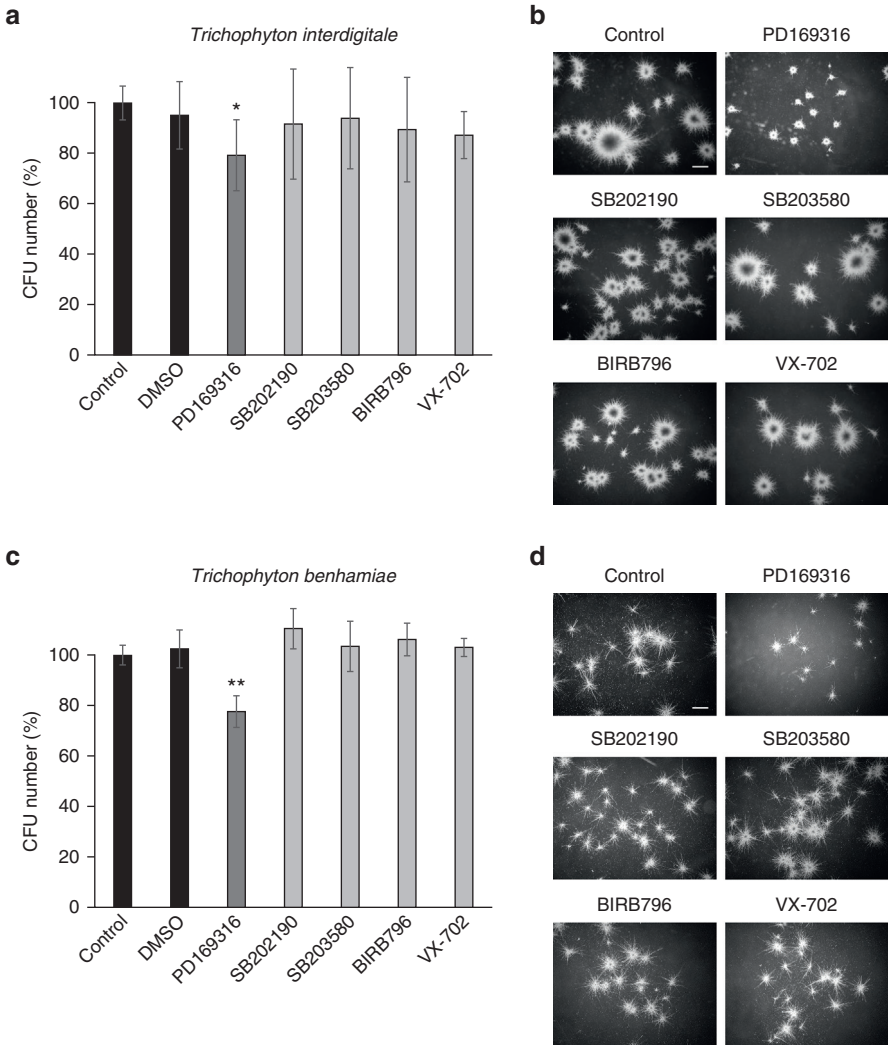

Supplementary Figure S6. Among five p38 MAPK inhibitors, PD169316 is the only one that impedes growth in other *Trichophyton* species. (**a, b**) *Trichophyton interdigitale* or (**c, d**) *Trichophyton benhamiae* arthroconidia were seeded on Sabouraud agar containing 15 μM of different p38 MAPK-specific inhibitors (PD169316, SB202190, SB203580, BIRB796, VX-702) or without inhibitors (Control) and incubated for 7 days at 27 °C. (**a**–**c**) Growth percentage calculated by counting CFUs (n = 3; mean ± standard deviation) and (**b**–**d**) by microscopic observation of colonies compared with control conditions. Scale bars = 1 mm. ***$P < 0.001$, Student *t* test. CFU, colony-forming unit; MAPK, mitogen-activated protein kinase.

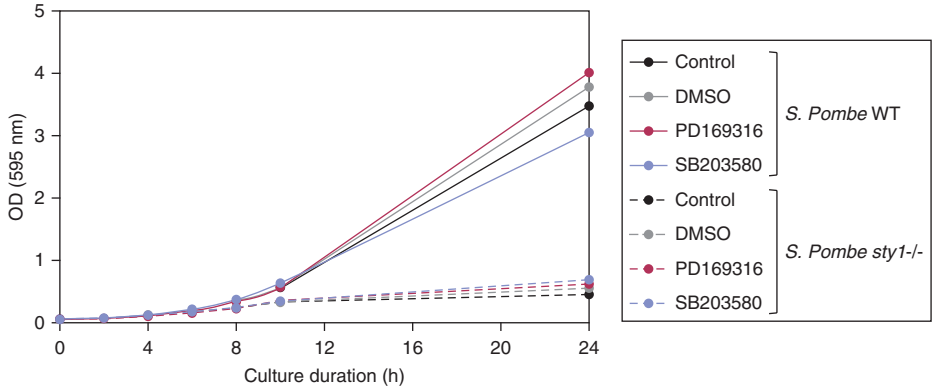

Supplementary Figure S7. PD169316 does not affect growth of *Schizosaccharomyces pombe*. WT or sty1$^{-/-}$ strains of *S. pombe* were cultured in liquid YES medium at 37 °C during 24 hours in presence or not of PD169316 (15 μM) or SB203580 (15 μM), or of DMSO (0.1%). Growth was monitored over time by measuring the OD at 595 nm 0, 2, 4, 6, 10, and 24 hours after culture beginning. DMSO, PD169316, or SB203580 were added in culture suspension after two hours. OD, optical density; sty1$^{-/-}$, *sty1* knockout; WT, wild-type.

Supplementary Table S1. Sequence of Primer Pairs Used for QRT-PCR

Gene Symbol	Forward Primer	Reverse Primer
FLG	GGGCACTGAAAGGCAAAAAG	CACCATAATCATAATCTGCACTACCA
hBD-2	ATCAGCCATGAGGGTCTTGT	GAGACCACAGGTGCCAATTT
hBD-3	TCCAGGTCATGGAGGAATCAT	CGAGCACTTGCCGATCTGT
IL-1α	AACCAGTGCTGCTGAAGGAGAT	TGGTCTCACTACCTGTGATGGTTT
IL-1β	TCCCCAGCCCTTTTGTTGA	TTAGAACCAAATGTGGCCGTG
IL-6	CCTGAACCTTCCAAAGATGGC	TTCACCAGGCAAGTCTCCTCA
IL-8	GCAGAGGGTTGTGGAGAAGTTT	TTGGATACCACAGAGAATGAATTTTT
IVL	TGAAACAGCCAACTCCAC	TTCCTCTTGCTTTGATGGG
LOR	TCATGATGCTACCCGAGGTTTG	CAGACCTAGATGCAGCCGGAGA
RNase 7	CGTGTCCCTGACCATGTGTAA	GACTTGTTCTGTCGCTTCTCTT
RPLP0	ATCAACGGGTACAAACGAGTC	CAGATGGATCAGCCAAGAAGG
S100A7	ACGTGATGACAAGATTGAGAAGC	GCGAGGTAATTTGTGCCCTTT
TGM1	GTCGTCTTCCGGCTCGAA	TCACTGTTTCATTGCCTCCAAT
TLR2	ATCCTCCAATCAGGCTTCTCT	GGACAGGTCAAGGCTTTTTACA
TLR5	TCCCTGAACTCACGAGTCTTT	GGTTGTCAAGTCCGTAAAATGC
TLR6	TTCTCCGACGGAAATGAATTTGC	CAGCGGTAGGTCTTTTGGAAC
TNFα	GAGGCCAAGCCCTGGTATG	CGGGCCGATTGATCTCAGC
TSLP	CGCGTCGCTCGCCAAAGAAA	TGAAGCGACGCCACAATCCTTG

Supplementary Table S2. Commercial ELISA Kits

Cytokine/ AMP	ELISA Kit
G-CSF	Human G-CSF DuoSet ELISA (R&D system, Abingdon, UK)
hBD-2	Human BD-2 Mini ABTS ELISA Development Kit (PeproTech, London, UK)
hBD-3	Human BD-3 Mini ABTS ELISA Development Kit (PeproTech, London, UK)
IL-1α	Human IL-1 alpha/IL1F1 DuoSet ELISA (R&D system, Abingdon, UK)
IL-1β	Human IL-1 beta/IL-1F2 DuoSet ELISA (R&D system, Abingdon, UK)
IL-8	Human IL-8/CXCL8 DuoSet ELISA (R&D system, Abingdon, UK)
IL-6	Human IL-6 DuoSet ELISA (R&D system, Abingdon, UK)
TNFα	Human TNF-alpha DuoSet ELISA (R&D system, Abingdon, UK)
TSLP	Human TSLP DuoSet ELISA (R&D system, Abingdon, UK)

Supplementary Table S3. Primary Antibodies Used for Western Blotting

Protein	Species	Company	Dilution
HSP27	Mouse	Cell Signaling Technology, Leiden, Netherlands	1/1000
Phospho-HSP27	Rabbit	Millipore, Overijse, Belgium	1/5000
p38 MAPK	Rabbit	Cell Signaling Technology, Leiden, Netherlands	1/1000
Phospho-p38 MAPK	Rabbit	Cell Signaling Technology, Leiden, Netherlands	1/1000
RPL13a	Rabbit	Cell Signaling Technology, Leiden, Netherlands	1/1000